Coastal Engineering Journal, Vol. 40, No. 1 (1998) 23–40

NUMERICAL COMPUTATIONS OF THE NONLINEAR ENERGY TRANSFER OF GRAVITY-WAVE SPECTRA IN FINITE WATER DEPTHS

NORIAKI HASHIMOTO, HIROICHI TSURUYA and YASUYUKI NAKAGAWA
Marine Environment Div., Port and Harbour Research Institute, Ministry of Transport, 3-1-1, Nagase, Yokosuka, 239-0826 Japan.

Received 21 April 1997

A new computational scheme for calculating the nonlinear energy transfer in finite-depth gravity wave spectra has been developed by extending the methods established by Masuda (1980) and Komatsu *et al.* (1993). In this paper, the formulations for the numerical computation of the nonlinear energy transfer for finite-depth water waves are shown with the analytical solution around the singular point of the Boltzmann integral. The numerical computational procedure for the proposed method is described in detail. Some results of numerical examinations for finite water depth, assuming two different types of directional spectra, are shown with discussions on the validity of the proposed method.

1. Introduction

Nonlinear wave-wave interactions are one of the most pervasive physical processes controlling the evolution and attenuation of waves during their propagation along the ocean surface. This mechanism causes the energy transfer among an infinite number of component waves, each of which has a different frequency and propagation direction. Recently, this process has been recognized to be as significant as the energy transfer from winds to waves and the energy dissipation by wave breaking. For these reasons, it has become one of the most critical research topics to further understand this physical process and incorporate this knowledge into wave forecasting and/or hindcasting models as accurately and efficiently as possible.

This mechanism was originally formulated by Hasselmann (1962) in the form of Boltzmann's integral. Boltzmann's integral, however, includes a complicated nonlinear kernel function and a singular point which makes the numerical integration difficult and unstable. Since the computation is very time consuming, there are very few investigations which have attempted to compute the nonlinear energy transfer for the realistic cases involving continuous directional spectra.

Among the recent examples, Hasselmann and Hasselmann (1981) reported the results for deep and finite water depth cases. Those results seem to be numerically unstable, however. Masuda (1980) developed an accurate computational method by

analytically deriving approximate solutions around the singular point of the Boltzmann integral. Masuda (1980) also presented some reliable computational results and provided comprehensive explanations on the characteristics of nonlinear wave-wave interactions of deep water waves.

Recently, Komatsu *et al.* (1993) developed an efficient computational method by modifying Masuda's method to take into consideration the symmetrical nature of nonlinear wave-wave interactions which were originally introduced by Hasselmann and Hasselmann (1981). This method makes the computation 300 times faster than Masuda's method while retaining most of Masuda's accuracy. Although Masuda's and Komatsu's methods are very accurate and stable computationally, they are restricted to deep water wave applications.

Web (1978) developed another accurate computational scheme by introducing a locus along which Boltzmann's integral is numerically integrated. Using this locus, obtained by removing the delta functions from the Boltzmann integral, the instability created by the singular point can be eliminated. Resio and Perrie (1990) modified Web's method by introducing the symmetries of the nonlinear wave-wave interactions. When both of these methods are incorporated into wave forecasting/hindcasting models, some difficulties arise since they include curvilinear coordinates (locus) rather than the physical coordinates of the time-space and frequency-direction domain.

Nonlinear interactions are an essential mechanism which always exist during the propagation of ocean surface waves but are hard to observe since they are usually compounded with other physical processes such as the evolution and attenuation of waves. It is, therefore, difficult to discuss the mechanism based solely on the data obtained by experiments and/or observations. For this reason, the theoretical approach is still indispensable to discuss the characteristics of the data. Komatsu's method seems to be superior to other existing methods such as Hasselmann's, Web's and Resio's with respect to accuracy, computation time and the ease with which it is incorporated into wave models. It has a disadvantage in that it is restricted to applications of deep water waves. Therefore, it is desirable to expand Komatsu's method for applications involving finite water depth waves. This new method would contribute to the understanding of the nonlinear wave-wave interactions and to the development of a reliable new generation of wave forecasting/hindcasting model.

This paper formulates the expanded theories of Masuda (1980) and Komatsu *et al.* (1993). This refined method has the advantage that it can be applied to deep and finite water depth waves. Some numerical results and discussions on the validity of the proposed method are also presented.

2. Formulation for Finite-Depth Gravity-Waves

The fundamental equation of the nonlinear energy transfer due to resonant wave-wave interactions was originally derived by Hasselmann (1962) which employed the

theoretical fifth-order perturbation analysis. This analysis yields a fourth-order effect comparable in magnitude to the growth and dissipation processes of ocean waves. The equation is known as the Boltzmann integral and is expressed by the following equation:

$$\frac{\partial n(\mathbf{k}_4)}{\partial t} = \int \cdots \int d\mathbf{k}_1 d\mathbf{k}_2 d\mathbf{k}_3 G(\mathbf{k}_1, \mathbf{k}_2, \mathbf{k}_3, \mathbf{k}_4) \times \delta(\mathbf{k}_1 + \mathbf{k}_2 - \mathbf{k}_3 - \mathbf{k}_4)\delta(\omega_1 + \omega_2 - \omega_3 - \omega_4) \times \{n_1 n_2 (n_3 + n_4) - n_3 n_4 (n_1 + n_2)\} \tag{1}$$

where, $n(\mathbf{k}_i) = \Phi(\mathbf{k}_i)/\omega_i$, $(i = 1, 2, 3, 4)$, is the action density of the two dimensional wave number spectrum, $\Phi(\mathbf{k}_i)$, for wave number $\mathbf{k}_i$ and angular frequency ω_i, $G(\mathbf{k}_1, \mathbf{k}_2, \mathbf{k}_3, \mathbf{k}_4)$ is the coupling coefficient (the nonlinear kernel function) and $\delta(\,)$ is the delta function representing the resonant conditions between four wave components:

$$\mathbf{k}_1 + \mathbf{k}_2 = \mathbf{k}_a = \mathbf{k}_3 + \mathbf{k}_4 \tag{2}$$

$$\omega_1 + \omega_2 = \omega_a = \omega_3 + \omega_4 \tag{3}$$

The wave number $\mathbf{k}_i$ and angular frequency ω_i, $(i = 1, 2, 3, 4)$ of the linear component waves satisfy the following dispersion relationship for the case of finite water depths.

$$\omega_i^2 = g k_i \tanh k_i h \tag{4}$$

where, g is the gravitational acceleration and h is the water depth. The nonlinear kernel function $G(\mathbf{k}_1, \mathbf{k}_2, \mathbf{k}_3, \mathbf{k}_4)$ is defined by:

$$G = \frac{9\pi g^2 D^2}{4\rho^2 \omega_1 \omega_2 \omega_3 \omega_4} \tag{5}$$

The quantity D has symmetries and has a very complicated form. The modification to the quantity D for the case of finite water depths was made by Herterich and Hasselmann (1980). The reader can refer to Hasselmann (1962) and Herterich and Hasselmann (1980) for details.

In the following, we expand on Masuda's formulation for deep water waves to the finite-depth gravity waves according to Masuda's derivation (1980). The symmetry of Eq. (1) with respect to $\mathbf{k}_1$ and $\mathbf{k}_2$ permits us to replace the integration over the entire $(\mathbf{k}_1, \mathbf{k}_2)$ space by that over the half-space where $|\mathbf{k}_1| \leq |\mathbf{k}_2|$. This results in:

$$\int d\mathbf{k}_3 \iint d\mathbf{k}_1 d\mathbf{k}_2 = 2 \int d\mathbf{k}_3 \iint_{|\mathbf{k}_1| \leq |\mathbf{k}_2|} d\mathbf{k}_1 d\mathbf{k}_2 \tag{6}$$

Hereafter, for simplicity, we will not explicitly write the conditions $|\mathbf{k}_1| \leq |\mathbf{k}_2|$, $\omega_1 \leq \omega_2$. Integration over $\mathbf{k}_2$ yields:

$$\frac{\partial n(\mathbf{k}_4)}{\partial t} = 2\int d\mathbf{k}_3 \int d\mathbf{k}_1 G(\mathbf{k}_1, \mathbf{k}_2, \mathbf{k}_3, \mathbf{k}_4)\delta(\omega_1 + \omega_2 - \omega_3 - \omega_4)$$
$$\times\{n_1 n_2(n_3 + n_4) - n_3 n_4(n_1 + n_2)\} \tag{7}$$

where $\mathbf{k}_2 = \mathbf{k}_3 + \mathbf{k}_4 - \mathbf{k}_1$ and $\omega_2 = \sqrt{gk_2 \tanh k_2 h}$. For practical applications, we can transform the above formula to that based on the frequency ω and the propagation direction θ. By use of the following relations:

$$d\mathbf{k} = \frac{k}{C_g(k)} d\omega d\theta \tag{8}$$

and

$$\frac{\Phi(\omega, \theta)}{\omega} d\omega d\theta = n(\mathbf{k}) d\mathbf{k}\,, \tag{9}$$

we have

$$\frac{\partial \Phi(\omega_4, \theta_4)}{\partial t} = \frac{2\omega_4 k_4}{C_g(k_4)} \iint d\omega_3 d\theta_3 \iint d\omega_1 d\theta_1 \left\{ \frac{k_1 k_3}{C_g(k_1) C_g(k_3)} G \right\}$$
$$\times\delta(\omega_1 + \omega_2 - \omega_3 - \omega_4)\{n_1 n_2(n_3 + n_4) - n_3 n_4(n_1 + n_2)\} \tag{10}$$

In order to clearly express the meaning of the resonant four wave interactions, a projection of the family of resonant loops in three dimensions of $(\mathbf{k}, \omega)$ onto the wave-number plane is often utilized as shown in Fig. 1. This specifies the sets of wave-numbers for surface waves capable of undergoing resonant interactions. If $\mathbf{k}_3$ and $\mathbf{k}_4$ are fixed, the resonant conditions determine $\mathbf{k}_1$ and $\mathbf{k}_2$ except for one degree of freedom from the resonant conditions, Eqs. (2) and (3). Although Longuet-Higgins (1962) specified the four resonant waves using the parameter $\gamma = \omega_a / \sqrt{gk_a}$, Masuda (1980) redefined it as $\gamma = \sqrt{gk_a}/\omega_a - 1/\sqrt{2}$ so that γ would be zero on the loop which passes through the center of the resonant interaction chart. It is clearly understood from Fig. 1 that for a given $\mathbf{k}_3$ and $\mathbf{k}_4$, $\mathbf{k}_1$ (or $\mathbf{k}_2$) must lie on a curve where $\gamma =$ constant. Using this parameter γ, Masuda skillfully derived the approximate solution around the singular point ($\gamma = 0$) of the Boltzmann integral to develop an accurate computational scheme for determining the nonlinear energy transfer for deep water gravity waves.

Now, we redefine the parameter γ by taking into consideration the effect of finite water depth as

$$\gamma = \sqrt{gk_a \tanh \frac{k_a}{2} h} \Big/ \omega_a - 1/\sqrt{2} \tag{11}$$

so that the parameter γ is zero at the singular points to be discussed later. When h is infinity, γ is identical to Masuda's definition.

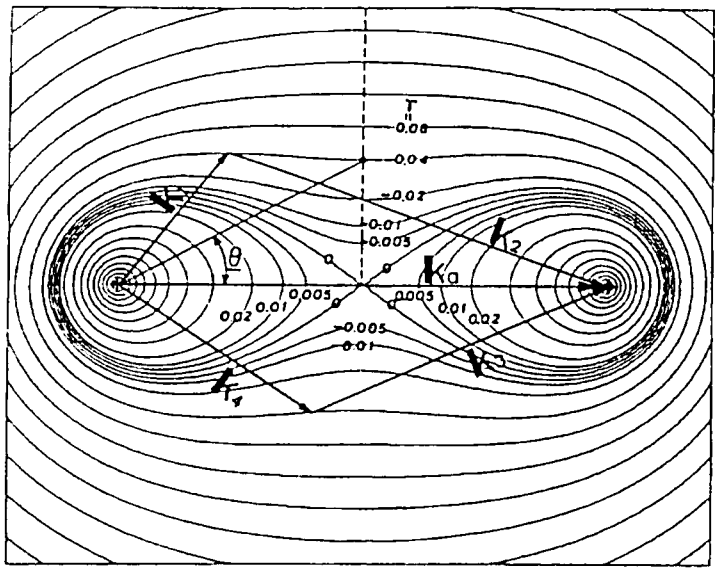

Fig. 1. Longuet-Higgins' interaction chart: contours of γ defined in Masuda (1980) for deep-water waves. (Masuda, 1980).

Following Masuda, we adopt $\theta_1 - \theta_a$ as a parameter representing the remaining one degree of freedom, where θ_a is the direction of $\mathbf{k}_a$ in Eq. (2). Then the frequency ω_1 is obtained by numerically solving Eqs. (2) and (3). By virtue of the condition $|\mathbf{k}_1| \leq |\mathbf{k}_2|$ or $\omega_1 \leq \omega_2$, the frequency ω_1 is determined uniquely. Details of the computation to obtain ω_1 will be discussed later. Note that for $\gamma < 0$ the condition $|\mathbf{k}_1| \leq |\mathbf{k}_2|$ restricts the range of $\theta_1 - \theta_a$ (see Fig. 1) as:

$$\Theta = \cos^{-1}\left(\frac{k_a}{2k_1}\right) \leq |\theta_1 - \theta_a| \leq \pi \tag{12}$$

Integrating Eq. (10) over ω_1 yields:

$$\frac{\partial \phi(\omega_4, \theta_4)}{\partial t} = \frac{2\omega_4 k_4}{C_g(k_4)} \iint d\theta_3 d\omega_3 \int d\theta_1 \times \left\{\frac{k_1 k_3}{C_g(k_1) C_g(k_3)} \frac{G}{S}\right\} \{n_1 n_2 (n_3 + n_4) - n_3 n_4 (n_1 + n_2)\} \tag{13}$$

where the denominator S, arising from $\delta(\omega_1 + \omega_2 - \omega_3 - \omega_4)$, is given by:

$$S = \left|1 + \frac{C_g(k_2)}{C_g(k_1)} \left\{\frac{k_1 - k_a \cos(\theta_1 - \theta_a)}{k_2}\right\}\right| \tag{14}$$

For convenience, we can write:

$$\tilde{\theta}_1 = \theta_1 - \theta_a, \quad \tilde{\theta}_2 = \theta_2 - \theta_a, \quad \tilde{\theta}_3 = \theta_3 - \theta_4 \tag{15}$$

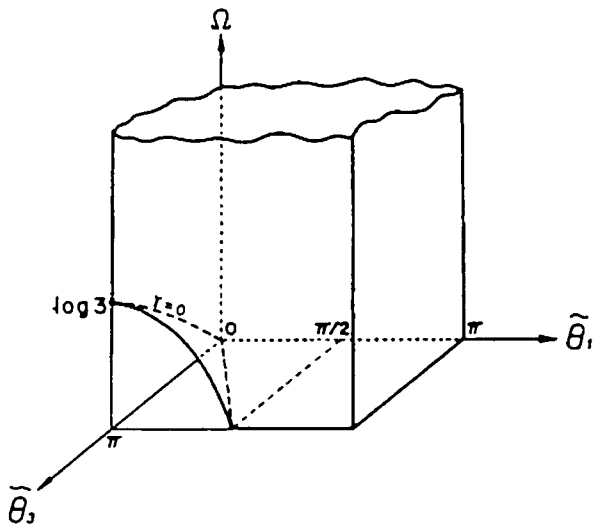

Fig. 2. A schmatic graph of the region over which the integration (17) is performed. (Masuda, 1980).

and

$$\Omega = \ln \omega_3 \tag{16}$$

Equation (13) can be transformed to the final formula to calculate the nonlinear energy transfer:

$$\begin{aligned}\frac{\partial \phi(\omega_4, \theta_4)}{\partial t} = \frac{2\omega_4 k_4}{C_g(k_4)} \int_0^{\pi} d\tilde{\theta}_3 \int_0^{\infty} d\Omega \int_0^{\pi} d\tilde{\theta}_1 \\ \times \sum_{\pm} \sum_{\pm} \sum_{\pm} \left\{ \frac{k_1 k_3 \omega_3}{C_g(k_1) C_g(k_3)} \frac{G}{S} \right\} \\ \times \{ n_1 n_2 (n_3 + n_4) - n_3 n_4 (n_1 + n_2) \}\end{aligned} \tag{17}$$

where:

$$\int_{-\pi}^{\pi} d\tilde{\theta}_3 \int_{-\infty}^{\infty} d\Omega \int_{-\pi}^{\pi} d\theta_1 \tag{18}$$

has been replaced by:

$$\int_0^{\pi} d\tilde{\theta}_3 \int_0^{\infty} d\Omega \int_0^{\pi} d\theta_1 \times \sum_{\pm} \sum_{\pm} \sum_{\pm} \tag{19}$$

Figure 2 schematically shows the domain of integration in the $(\tilde{\theta}_1, \Omega, \tilde{\theta}_3)$ space. It is an infinitely long rectangular prism excluding a lower region resulting from the condition $\omega_1 \leq \omega_2$. This excluded volume is bounded by three planes; $\tilde{\theta}_3 = \pi$, $\Omega = 0$, $\tilde{\theta}_1 = 0$, and a curved surface $\tilde{\theta}_1 = \Theta(\tilde{\theta}_3, \Omega)$.

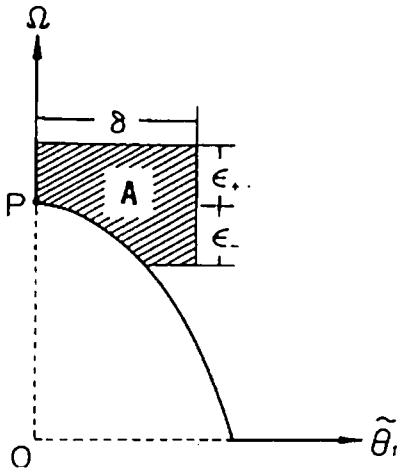

Fig. 3. A schematic graph of a cross section ($\tilde{\theta}_3$ = constant) of the rectangular prism in Fig. 2. (Masuda, 1980).

As Masuda noted, the singularity in Eq. (17) comes from S only. Simple manipulation yields:

$$S = \left| 1 \pm \frac{C_g(k_2)}{C_g(k_1)} \left\{ 1 - \frac{k_a^2}{k_2^2} \sin^2 \tilde{\theta}_1 \right\}^{1/2} \right| \tag{20}$$

By virtue of the condition of $\omega_1 \leq \omega_2$, S vanishes only when $\omega_1 = \omega_2$ and $\tilde{\theta}_1 = 0$. That is, the singular points are located along a curve $\gamma = 0$ on the plane $\tilde{\theta}_1 = 0$ (see Fig. 2). Therefore, special treatment is necessary to perform the integration of Eq. (17) around the singular point $\gamma = 0$.

Although we introduced the transformation in terms of direction, θ, only in Eq. (15) for the convenience of numerical computations, Masuda also introduced the transformation for frequency, ω, by dividing ω by the target frequency, ω_4, at which the nonlinear energy transfer is to be calculated. Although Masuda's transformation can reduce the computational time to a large degree for deep water waves, this benefit is not valid for finite water waves. This issue will be discussed presently.

3. Integration Around the Singular Point

In this section an analytical integral of Eq. (17) around the singular point is derived according to Masuda (1980). Equation (17) is carried out successively in the order of $\tilde{\theta}_1$, Ω, $\tilde{\theta}_3$. Therefore, we must integrate Eq. (17) first on the plane $\tilde{\theta}_3$ = constant. The singular point is denoted by P in Fig. 3. The integration over the area A surrounding P is to be calculated analytically, where A is defined by $\Theta \leq \tilde{\theta}_1 \leq \delta$,

and $-\varepsilon_- \leq \Omega - \Omega_P \leq \varepsilon_+$. We can rewrite the integration as:

$$\iint_A d\Omega d\tilde{\theta}_1 \frac{R}{S} \approx R_P \iint_A d\Omega d\tilde{\theta}_1 \frac{1}{S_P} \tag{21}$$

where

$$R = \frac{k_1 k_3 \omega_3 G}{C_g(k_1) C_g(k_3)} \{n_1 n_2 (n_3 + n_4) - n_3 n_4 (n_1 + n_2)\} \tag{22}$$

is the numerator, R_P is the value of R at the singular point P, and S_P is given by

$$S_P = \sqrt{-\frac{2k_a D_g(k_a/2)}{C_g(k_a/2)} \tilde{\theta}_1^2 - \frac{4\sqrt{2}\omega_a D_g(k_a/2)}{\{C_g(k_a/2)\}^2} \mu(\Omega - \Omega_p)} \tag{23}$$

where $D_g(k) = \partial C_g(k)/\partial k$, and

$$\begin{aligned} \mu &= \left(\frac{\partial \gamma}{\partial \Omega}\right)_P = \left(\omega_3 \frac{\partial \gamma}{\partial \omega_3}\right)_{\gamma=0} \\ &= \frac{\omega_3}{\sqrt{2}\omega_a} \left\{ \frac{C_g(k_a/2)}{C_g(k_3)} \frac{k_3 + k_4 \cos\tilde{\theta}_3}{k_a} - 1 \right\} \end{aligned} \tag{24}$$

Equation (23) can be derived after some manipulation of Eq. (14) using the conditions of $k_1/k_2 = 1 - \Delta$, $|\Delta| \ll 1$, and $|\theta_1| \ll 1$, $|\theta_2| \ll 1$ around the singular point P.

Referring to Fig. 3, the integration of Eq. (21) can be performed by separating the area A as

$$\iint_A d\Omega d\tilde{\theta}_1 \frac{1}{S_P} = \int_{-\varepsilon_-}^{0} d\Omega \int_{\Theta}^{0} d\tilde{\theta}_1 \frac{1}{S_P} + \int_0^{\varepsilon_+} d\Omega \int_0^{\delta} d\tilde{\theta}_1 \frac{1}{S_P} \tag{25}$$

Since the lower limit Θ of the integral in terms of $\tilde{\theta}_1$ in the first term of the right hand side of Eq. (25) can be approximated around $\gamma \approx 0$ by

$$\Theta = \sqrt{-\frac{2\sqrt{2}\omega_a}{k_a C_g(k_a/2)} \mu(\Omega - \Omega_p)}\,, \tag{26}$$

then, the integration of Eq. (25) can be obtained

$$\begin{aligned} \iint_A d\Omega d\tilde{\theta}_1 \frac{1}{S_P} = {} & \frac{\varepsilon_+}{\sqrt{a}} \ln \frac{|\sqrt{a}\delta + \sqrt{a\delta^2 + b\varepsilon_+}|}{|\sqrt{b\varepsilon_+}|} - \delta \frac{\sqrt{a}\delta - \sqrt{a\delta^2 + b\varepsilon_+}}{b} \\ & + \frac{\varepsilon_-}{\sqrt{a}} \ln \frac{|\sqrt{a}\delta + \sqrt{a\delta^2 - b\varepsilon_-}|}{|(\sqrt{ac} + \sqrt{ac - b})\sqrt{\varepsilon_-}|} + \delta \frac{\sqrt{a}\delta - \sqrt{a\delta^2 - b\varepsilon_-}}{b} \end{aligned} \tag{27}$$

where

$$\left.\begin{aligned} a &= -\frac{2k_a D_g(k_a/2)}{C_g(k_a/2)}, \quad b = -\frac{4\sqrt{2}\omega_a D_g(k_a/2)}{\{C_g(k_a/2)\}^2} \\ c &= \frac{2\sqrt{2}\omega_a}{k_a C_g(k_a/2)}\mu \end{aligned}\right\} \tag{28}$$

The above argument ceases to be valid near the zero-point of $\mu = (\partial\gamma/\partial\Omega)_P$, which is found at the origin, $\tilde{\theta}_3 = \Omega = \tilde{\theta}_1 = 0$. This kind of singularity can be treated only by calculating a triple integral as Masuda derived for deep water waves. However, when the computation method discussed in the following section is utilized, it is not necessary to take into consideration this singularity since the contribution from this singularity is canceled out at the point where the resonant four waves have the same wave number vectors.

The derivation of the extended computational method of Masuda (1980) was described for finite-depth gravity waves. It is easily confirmed that all the equations and variables derived above are identical to Masuda's derivations when the water depth h is infinity.

4. Methodology of the Numerical Computation of Nonlinear Energy Transfer

In order to carry out the numerical computations using the equations derived in the previous sections, we utilized Komatsu's method. Komatsu *et al.* (1993) made use of the resonant interaction symmetries, as in Hasselmann and Hasselmann (1981) and Resio and Perrie (1991), and truncated less significant configurations of resonance to achieve shorter computational time without serious loss of accuracy.

As Komatsu *et al.* (1993) mentioned, there are two kinds of symmetries in the resonant interaction. The first is based on the well-known nature of nonlinear resonant interactions among gravity waves expressed by the integral formula of Eq. (1). Consider a particular combination of four resonant waves with wave number vector $\mathbf{k}_i (i = 1, 2, 3, 4)$. As explained in Hasselmann and Hasselmann (1981), $\delta n(\mathbf{k}_i) d\mathbf{k}_i/\delta t (i = 1, 2, 3, 4)$ have the following relationship:

$$\frac{\delta n(\mathbf{k}_1)}{\delta t} d\mathbf{k}_1 = \frac{\delta n(\mathbf{k}_2)}{\delta t} d\mathbf{k}_2 = -\frac{\delta n(\mathbf{k}_3)}{\delta t} d\mathbf{k}_3 = -\frac{\delta n(\mathbf{k}_4)}{\delta t} d\mathbf{k}_4 \tag{29}$$

where $\delta n(\mathbf{k})/\delta t$ indicates the action transfer that is due to this particular resonance combination. As shown in Eq. (29), $\delta n(\mathbf{k}_i) d\mathbf{k}_i/\delta t (i = 1, 2, 3, 4)$ are of equal magnitude but are different in sign. The outer pair of frequencies consist of the highest and lowest frequencies of the four resonant wave components. The inner pair of frequencies consist of the remaining two components. The resonance interaction deprives energy from the inner pair to supply it to the outer pair, and vice versa (Masuda,

1986). Accordingly, if we calculate $\delta n(\mathbf{k})/\delta t$ for one component of the resonant four waves, then we immediately know $\delta n(\mathbf{k})/\delta t$ for the other three components.

The second type of symmetry is associated with the geometrical similarity of resonance configurations. One is the mirror image of a resonance combination which has the same interaction coefficient as the original one. The other is a rotation of a resonance combination which also gives the same interaction coefficient.

Masuda (1980) and Komatsu *et al.* (1993) made use of another symmetry, a scale transform of wave numbers, which preserves the resonance condition. As mentioned in Masuda (1980) for the case of deep water waves, if we specify a particular wave number vector $\mathbf{k}_4(\omega_4$ and $\theta_4)$ at which the nonlinear energy transfer is to be evaluated, and normalize the variables such as $G, S, \omega_1, \ldots$ in the Boltzmann integral by the specific wave number $\mathbf{k}_4$, those variables do not depend on the magnitude or the direction of the wave number vector $\mathbf{k}_4$. They are determined by the configuration of wave vectors of resonant waves regardless of the specific wave $\mathbf{k}_4$. In other words, they are functions of $\tilde{\theta}_3 = \theta_3 - \theta_4$, $\tilde{\Omega} = \ln(\omega_3/\omega_4)$ and $\tilde{\theta}_1 = \theta_1 - \theta_a$ only. Therefore, this normalization makes it sufficient to calculate the complicated functions $G, S, \omega_1, \ldots$ only once in advance, which reduces the computational time to a large extent. Conversely, for finite-depth gravity waves, the above normalization is not valid, and the variables $G, S, \ldots$ depend not only on $\tilde{\theta}_3, \tilde{\Omega}, \tilde{\theta}_1$ but also on ω_4. This is a reason why we have introduced the normalization only for the direction θ in Eq. (15). This property for finite water waves makes it time consuming to numerically integrate Boltzmann's integral since those variables are needed to be calculated for each specific frequency ω_4 for the target directional wave spectrum $\Phi(\omega_4, \theta_4)$.

In order to make use of the symmetries mentioned above, the (ω, θ) space is divided into bins of nonuniform finite areas in the same way as Masuda (1980) and Komatsu *et al.* (1993). The central frequency ω_I of each bin is distributed on a logarithmic scale from the minimum frequency, $\omega_{\min}$, to the maximum frequency, $\omega_{\max}$, at a constant ratio

$$R_\omega = \exp\{\Delta(\ln \omega)\} \tag{30}$$

as

$$\omega_{I+1} = R_\omega \omega_I \tag{31}$$

while the central direction, θ_J, of the bin is distributed as

$$\theta_{J+1} = \theta_J + \Delta\theta \tag{32}$$

with the directional increment $\Delta\theta$ kept constant. By virtue of this distribution of bins, the second kind of symmetry is expressed as follows. If a combination of any four bins satisfies the resonance condition, so do any combinations of the four bins that are obtained from the original combination through (1) mirror transform and (2) rotational transform. The scale transform utilized in Masuda (1980) and

Komatsu *et al.* (1993) for deep water waves cannot be used in finite-depth water waves as mentioned before. In the following, bin (ω_I, θ_J) are referred to as (I, J).

Now, we specify a particular wave number vector $\mathbf{k}_4(\omega_4$ and $\theta_4)$ at which the nonlinear energy transfer is to be evaluated, and assume the order of magnitude of frequencies as follows considering the first kind of symmetry of the nonlinear wave-wave interaction.

$$\omega_3 \leq \omega_1 \leq \omega_2 \leq \omega_4 \tag{33}$$

For the computation of realistic continuous energy transfer $\partial n(\omega_4, \theta_4)/\partial t$, the computation must be carried out with the loops of frequency ω_4 and direction θ_4, where the outer loop is ω_4 and inner loop is θ_4. Between the two loops, the computation of the configuration of resonant interactions for each frequency are performed with the computation of variables such as $G, S, \ldots$ in the Boltzmann integral for both regular and singular points. In the inner loop of direction θ_4, the computation of nonlinear energy transfer for each direction θ_4 is carried out using the resonant configuration with the symmetries of the configuration.

Since the efficient method utilizing symmetries is described in Komatsu *et al.* (1993) and Komatsu and Masuda (1996) in detail, the outline of the computation procedure is described in the following section for finite-depth water waves.

4.1. *Computation around the singular point*

This computation is to be carried out between the loop of frequency ω_4 and that of direction θ_4. Choose the variable $\tilde{\theta}_3$ as a parameter of the loop computation. By making use of the mirror image symmetry, the range of $\tilde{\theta}_3$ is assumed as $0 \leq \tilde{\theta}_3 \leq \pi$. Also, by making use of the rotational symmetry, θ_4 is assumed to be zero. Then, the following computation is carried out in the loop of $\tilde{\theta}_3$.

(1) Search for $\Omega_P(= \ln \omega_3)$ which satisfies $\gamma = 0$ and the condition of Eq. (33). This solution can be obtained by the iterative computation applying regula falsi (rule of false position) for $F_1(k_3) = 0$, where

$$F_1(k_3) = \frac{\omega_a^2}{2} - g k_a \tanh \frac{k_a h}{2} \tag{34}$$

$$\omega_a = \sqrt{g k_3 \tanh k_3 h} + \sqrt{g k_4 \tanh k_4 h} \tag{35}$$

$$k_a = \sqrt{k_3^2 + k_4^2 + 2 k_3 k_4 \cos \tilde{\theta}_3} \tag{36}$$

From the above computations, k_3, ω_3, k_a and ω_a can be obtained from the known values of ω_4, k_4, θ_4 and $\tilde{\theta}_3$.

(2) From the resonant condition, $\omega_1 = \omega_2 = \omega_a/2$ and $\tilde{\theta}_1 = \tilde{\theta}_2 = 0$ are obtained. From the computation of Steps (1) to (2), the resonant configuration at the singular point can be determined.

(3) Compute $\hat{\Omega}_P = |\Omega_P/\Delta\Omega| - [|\Omega_P/\Delta\Omega|]$, where $\Delta\Omega = \Delta(\ln\omega)$ and [ ] is the Gaussian notation of the maximum integer which does not exceed the real argument. When $\hat{\Omega}_P < 0.5$, the width of Ω of the infinitesimal area A in Fig. 3 is defined as:

$$\varepsilon_+ = (0.5 - \hat{\Omega}_P) \times \Delta\Omega \quad \text{and} \quad \varepsilon_- = (\hat{\Omega}_P + 0.5) \times \Delta\Omega \tag{37}$$

When $\hat{\Omega}_p \geq 0.5$, the point P is dealt with as a regular point.

(4) Using the analytical solution of Eq. (27), compute the following kernel function P

$$P = k_1 k_3 G/\{C_g(k_1)C_g(k_3)\} \iint_A d\Omega d\tilde{\theta}_1 (1/S_P) \tag{38}$$

where δ in Eq. (27) is set to be 1.5 $\Delta\theta$ according to Masuda (1980).

(5) By utilizing the second kind of symmetry, compute the relative coordinate $(I_k, \tilde{J}_k)$ of the bin for the resonant three other waves $(\omega_i, \theta_i)(i = 1, 2, 3)$ to the target wave (ω_4, θ_4) by

$$\tilde{J}_k = J_k - J_4 (k = 1, 2, 3)\,. \tag{39}$$

The relative coordinates of the bins for each symmetry configuration are related to the original configuration and are preserved with the value of the kernel function P for the computation of the nonlinear energy transfer discussed presently.

It should be noted that, in order to limit the number of resonance combinations, we discard the resonance configurations for which the ratio of the higher and lower frequencies of ω_4/ω_3 exceeds a prescribed value of $C_r(= 3.0)$ according to Komatsu *et al.* (1993). As mentioned previously, it is not necessary to take into consideration the singularity at the origin since the contribution from this singularity is canceled out at the point where the resonant four waves have the same wave numbers.

4.2. *Computation at the regular point*

This computation is to be carried out between the loop of frequency ω_4 and that of direction θ_4. Choose the variables $\tilde{\theta}_3, \omega_3$, and $\tilde{\theta}_1$ as parameters of the loop computations. By making use of the mirror image symmetry, the ranges of $\tilde{\theta}_3$ and $\tilde{\theta}_1$ are assumed as $0 \leq \tilde{\theta}_3 \leq \pi$ and $\Theta \leq \tilde{\theta}_1 \leq \pi$, respectively. Also, by making use of the rotational symmetry, θ_4, is assumed to be zero. Then, the following computation is carried out in the loops of $\tilde{\theta}_3$, ω_3 and $\tilde{\theta}_1$ in this order.

(1) Search for ω_1, ω_2 and $\tilde{\theta}_2$ satisfying the condition of Eq. (33). The solutions can be obtained by the iterative computation applying regula falsi for $F_2(k_1) = 0$,

where

$$F_2(k_1) = \omega_a - \sqrt{gk_1 \tanh k_1 h} - \sqrt{gk_2 \tanh k_2 h} \tag{40}$$

$$k_2 = \sqrt{k_a^2 + k_1^2 - 2k_a k_1 \cos\tilde{\theta}_1} \tag{41}$$

$$\tilde{\theta}_2 = \tan^{-1}\left\{\frac{-k_1 \sin\tilde{\theta}_1}{k_a - k_1 \cos\tilde{\theta}_1}\right\} \tag{42}$$

By the above computation, k_1, k_2 and $\tilde{\theta}_2$ can be obtained from the known values of $\omega_4, k_4, \theta_4, \tilde{\theta}_3, \omega_3$ and $\tilde{\theta}_1$ to get the resonant configuration at the regular point.

(2) Compute the following kernel function K

$$K = k_1 k_3 \omega_3 G/\{C_g(k_1)C_g(k_3)S\} \tag{43}$$

(3) Compute the relative coordinate $(I_k, \tilde{J}_k)$ of the bin for the remaining three resonant waves $(\omega_i, \theta_i)(i = 1, 2, 3)$ to the target wave (ω_4, θ_4) by Eq. (39). The relative coordinates of the bins for each symmetry configuration are related to the original configuration and are preserved with the value of the kernel function K for the computation of the nonlinear energy transfer discussed presently.

It should be noted that we also discard the resonance configurations for which the ratio of the higher and lower frequencies of ω_4/ω_3 exceeds a prescribed value of $C_r(= 3.0)$ according to Komatsu *et al.* (1993). This convention is the same as that adopted for the computation around the singular point.

4.3. *Computation of the nonlinear energy transfer*

The action density, $n(I, J) = \Phi(I, J)C_g/(\omega k)$, is obtained from the directional spectrum $\Phi(I, J) = \Phi(\omega, \theta)$. Using the relative configuration $(I_k, \tilde{J}_k)$ to the wave (I_4, J_4) previously obtained, the following computation is to be carried out for each (ω_4, θ_4) in the inner loop of direction θ_4. That is, in the inner loop of direction θ_4, the computations of the following steps (1) to (3) are repeated for all the configurations including the symmetries of both the singular and the regular points.

(1) Compute the coordinates of waves $(I_k, J_k)(k = 1, 2, 3)$ by

$$J_k = \tilde{J}_k + J_4(k = 1, 2, 3)\,. \tag{44}$$

(2) Using the action density, $n_k = n(I_k, J_k)(k = 1, 2, 3)$, compute the following integrand for the regular point and singular point, respectively.

$$dW_p = 2\omega_4 k_4 P/C_g(k_4)\{n_1 n_2(n_3 + n_4) - n_3 n_4(n_1 + n_2)\}\Delta\tilde{\theta}_3 \Delta\Omega \Delta\tilde{\theta}_1 \tag{45}$$

$$dW_k = 2\omega_4 k_4 K/C_g(k_4)\{n_1 n_2(n_3 + n_4) - n_3 n_4(n_1 + n_2)\}\Delta\tilde{\theta}_3 \tag{46}$$

(3) Accumulate the rate of the action density, Δn_k, for each related bin of the wave component $(I_k, J_k)(k = 1, 2, 3, 4)$ by

$$\begin{Bmatrix} \Delta n_1 \\ \Delta n_2 \\ \Delta n_3 \\ \Delta n_4 \end{Bmatrix} = \begin{Bmatrix} -1 \\ -1 \\ 1 \\ 1 \end{Bmatrix} \begin{Bmatrix} dW_K \\ dW_P \end{Bmatrix} \tag{47}$$

5. Analysis of Result

Since the proposed method derived herein is a generalized method including the methods of Masuda (1980) and Komatsu *et al.* (1993), it can accurately and smoothly simulate the nonlinear energy transfer for deep water waves even when a rough mesh size is applied such as 24 × 36 in the frequency and direction domain, respectively. No significant difference can be seen between the results of the proposed method and those of Masuda (1980) and Komatsu *et al.* (1993) for deep water waves.

However, for the case of finite-depth gravity waves, especially $k_P h \approx 1$, where k_P is the wave number corresponding to the peak frequency of the power spectrum, such rough mesh sizes make the computational results unstable and produce a "zigzag" shape in the nonlinear energy transfer.

In the following, the characteristics of nonlinear energy transfer are examined in one dimensional form $T_1(\omega)$ defined by:

$$T_1(\omega) = \int \frac{\partial \Phi(\omega, \theta)}{\partial t} d\theta \tag{48}$$

Figure 4 shows examples of the nonlinear energy transfer for $k_P h = 10.0$, 1.0 and 0.8, where the wave spectra examined are the Pierson-Moskowitz spectrum (which will be abbreviated as the PM spectrum hereafter) and the JONSWAP spectrum, respectively, with a $\cos^2\theta$ directional spreading function. The peak frequency of each power spectrum is chosen as $\omega_P = 1$, and the mesh size for the numerical computation is 72 × 96 in the frequency and direction domains, respectively.

As shown in Fig. 4, the characteristics of the nonlinear energy transfer are different in each case depending on the shape of the directional spectrum and the magnitude of the relative water depth $k_P h$. For the case of the PM spectrum, the result for $k_P h = 10.0$ shows the maximum value of the nonlinear energy transfer around the peak frequency, ω_P, of the spectrum, and the minimum value around $1.5\omega_P$. However, when $k_p h$ decreases to smaller values of finite water depth, i.e. smaller than $k_P h \approx 1$, the location of the maximum and the minimum value of the nonlinear energy transfer shifts toward the lower frequency side and the magnitude of their absolute values are increased.

For the case of the JONSWAP spectrum, the result for $k_P h = 10.0$ shows the maximum value of the nonlinear energy transfer around $0.95\omega_P$, and the minimum

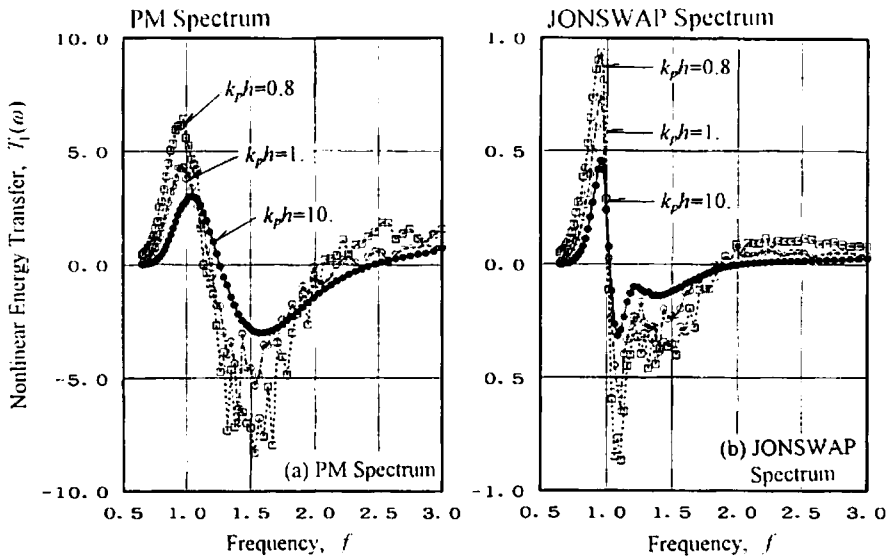

Fig. 4. Comparison of the one dimensional nonlinear energy transfer, $T_1(\omega)$, calculated for various k_ph as a parameter: (a) PM Spectrum, (b) JONSWAP Spectrum.

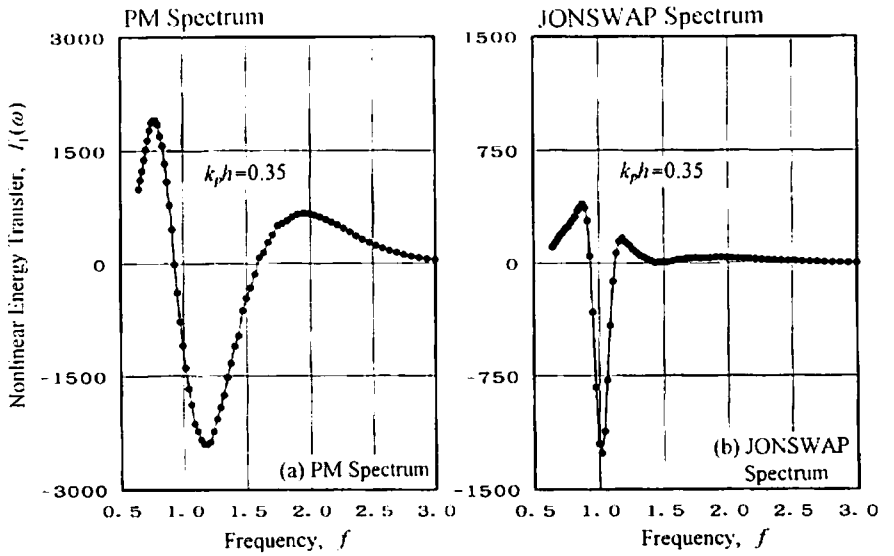

Fig. 5. Examples of the one dimensional nonlinear energy transfer, $T_1(\omega)$, calculated for $k_ph = 0.35$: (a) PM Spectrum, (b) JONSWAP Spectrum.

value around $1.1\omega_P$. These results are different from the case of the PM spectrum. In finite water depths, where $k_Ph \approx 1$, the locations of the maximum and the minimum values appear to be at the same location as that of $k_Ph = 10.0$. Their magnitudes, however, are also increased while maintaining the similar shape of $k_Ph = 10.0$.

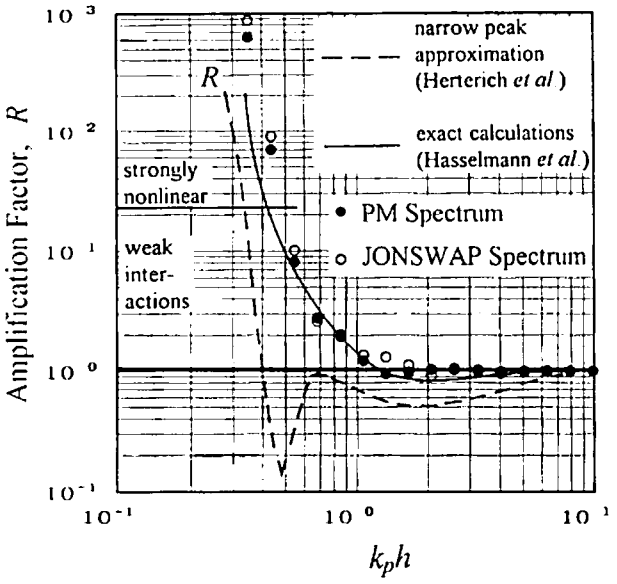

Fig. 6. Amplification factor R of the nonlinear energy transfer for finite-depth and infinite-depth wave spectra.

As Hasselmann and Hasselmann (1985) noted, for $k_p h \leq 0.4$, the nonlinear energy transfer exceeds the deep water values by more than an order of magnitude, and the weakly nonlinear approximation becomes questionable. For reference, however, Figs. 5 (a) and (b) show examples for $k_p h = 0.35$. The smooth shapes of the nonlinear energy transfer and the remarkable increases in their absolute values, which have different shapes depending on the assumed directional spectra, can be easily seen.

Figure 6 shows the comparison of the amplification factor of the nonlinear energy transfer for the finite-depth and the deep water waves. The circles in Fig. 6 are calculated by the following definition as a function of $k_p h$.

$$R(k_p h) = S_{\mathrm{nl}}(k_p h)_{\mathrm{peak}} / S_{\mathrm{nl}}(\infty)_{\mathrm{peak}} \tag{49}$$

where, $S_{\mathrm{nl}}(k_p h)_{\mathrm{peak}}$ is the maximum (peak) value of the nonlinear energy transfer calculated for a parameter of $k_p h$ with a specified directional spectrum. In Fig. 6, • and o show the differences of the assumed power spectrum, i.e., the PM spectrum and the JONSWAP spectrum, respectively. The solid and broken lines in Fig. 6 are results obtained from Hasselmann and Hasselmann (1981, 1985). Although Hasselmann and Hasselmann (1981, 1985) obtained these lines through numerical computations by assuming a Mitsuyasu-Hasselmann type directional spreading function, and they are different from our computational conditions, the results in Fig. 6 are generally in good agreement. The third generation wave forecasting/hindcasting model (WAM model; WAMDI Group, 1988) utilizes the amplification factor shown by the solid line in Fig. 6. The WAM calculates the nonlinear energy transfer in finite water depths

by simply multiplying the amplification factor by the result for deep water waves. Although the amplification factor in Fig. 6 seems to have no significant difference for the two types of power spectra (the PM and JONSWAP spectrum), we should note that there are actually significant differences in the shapes and the peak locations of the nonlinear energy transfer depending on the two assumed directional spectra.

Comparing the difference between the results of the proposed method and those of Hasselmann and Hasselmann (1981), the proposed method seems to have equivalent or better accuracy than that of Hasselmann and Hasselmann, since their results includes unstable "zigzag" shapes even for the case of deep water waves.

6. Concluding Remarks

The physical processes involved with the evolution and attenuation of waves propagating on the sea surface are very complicated. One of the most important processes is the nonlinear energy transfer among an infinite number of component waves. The formulation of this process was originally established by Hasselmann (1962) more than 30 years ago. However, the complexity and difficulty associated with numerical computations prevent us from fully understanding the mechanisms of the nonlinear energy transfer for various real sea conditions.

In this paper, we expanded Masuda's rigorous theory (1980) and Komatsu's efficient method (1993) for the cases of finite-depth gravity water waves. This method can be applied for various realistic sea conditions. The method was applied to some examples of common wave spectra in finite water depths. Some characteristics of the nonlinear energy transfer in finite water depths were clarified. Future research will include applying this method to various directional wave spectra in different water depths and investigating the characteristics of the nonlinear energy transfer more closely. We hope this paper will contribute to the understanding of the nonlinear energy transfer, and to the development of a new generation wave forecasting /hindcasting model.

Acknowledgements

We wish to express our sincere gratitude to Professor Akira Masuda and Dr. Kosei Komatsu of the Research Institute for Applied Mechanics, Kyushu University, for their valuable comments for this work. We are also very grateful to Mr. Sidney Walter Thurston III for his critical review and valuable comments on this paper.

References

Hasselmann, K.(1962). On the non-linear energy transfer in a gravity-wave spectrum, Part 1, General theory, J. Fluid Mech. **12**: 481–500.

Hasselmann, S. and Hasselmann, K. (1981). A symmetrical method of computing the nonlinear transfer in a gravity wave spectrum, Hamb. Geophys. Einzelschriften, Reihe A: Wiss. Abhasand. **52**: 138.

Hasselmann, S. and Hasselmann, K. (1985). Computations and parameterizations of the nonlinear energy transfer in a gravity-wave spectrum. Part I: A new method for efficient computations of the exact nonlinear transfer integral, J. Phys. Oceanogr. **15**: 1378–1391.

Herterich, K. and Hasselmann, K. (1980). A similarity relation for the nonlinear energy transfer in a finite-depth gravity-wave spectrum, J. Fluid Mech. **97**: 215–224.

Masuda, A. (1980). Nonlinear energy transfer between wind waves, J. Phys. Oceanogr. **10**: 2082–2092.

The WAMDI Group (13 Authors) (1988). The WAM model — A third generation ocean wave prediction model, J. Phys. Oceanogr. **18**: 1378–1391.

Komatsu, K., Kusaba, T. and Masuda, A. (1993). An efficient method for computing nonlinear energy transfer among wind waves, Bull. Res. Inst. Appl. Mech. Kyushu Univ. **75**: 121–146 (Japanese).

Komatsu, K. and Masuda, A. (1996). A new scheme of nonlinear energy transfer among wind waves: RIAM method — algorithm and performance —, J. Oceanogr. **52**: 509–537.

Longurt-Higgins (1962). Resonant interactions between two trains of gravity waves, J. Fluid Mech. **12**: 321–332.

Resio, D. and Perrie, W. (1991). A numerical study of nonlinear energy fluxes due to wave-wave interactions, J. Fluid Mech. **223**: 603–629.

Webb, D. J. (1978). Non-linear transfers between sea waves, Deep-Sea Res. **25**: 279–298.